Journal of Engineering Science and Technology
Vol. 18, No. 2 (2023) 1363 - 1379

ADSORPTION ISOTHERM CHARACTERISTICS OF CALCIUM CARBON MICROPARTICLES PREPARED FROM CHICKEN BONE WASTE TO SUPPORT SUSTAINABLE DEVELOPMENT GOALS (SDGS)

ASEP BAYU DANI NANDIYANTO*, RISTI RAGADHITA, MELI FIANDINI, RINA MARYANTI, DWI NOVIA AL HUSAENI, DWI FITRIA AL HUSAENI

Universitas Pendidikan Indonesia
*Corresponding Author: nandiyanto@upi.edu

Abstract

This work analyzed the adsorption isotherm on dye removal in an aqueous solution using calcium carbonate fabricated from chicken bone waste. In this study, an investigation of the adsorption isotherm model was carried out using a batch technique, in which curcumin was used as a dye model adsorbed under constant pH, pressure, and temperature. Adsorption results were then evaluated using ten adsorption isotherm models, including Langmuir, Freundlich, Temkin, Dubinin-Radushkevich, Fowler-Guggenheim, Hill-Deboer, Jovanovic, Harkin-Jura, Flory-Huggins, and Halsey. In addition, the fabricated calcium carbonate characterization process was also analyzed using a sieve test, digital microscope, and Fourier transforms infrared instrument. The result shows that several models are suitable to represent adsorption equilibrium if taken from the correlation coefficient value > 0.90 respectively, namely the Jovanovic, Hill-Deboer, Fowler-Guggenheim, Temkin, Flory-Huggins, and Dubinin-Radushkevich isotherms. The adsorption process indicated the formation of multilayers on a heterogeneous surface. Then, the adsorption process occurs normally, spontaneously, and favorably with the interaction between the adsorbate molecules being physical interaction. Calcium carbonate from chicken bone waste has an adsorption capacity of 4.582 mg/g. Based on this study, the adsorption process is endothermic and spontaneous. The findings indicate that an alternative calcium carbonate material derived from chicken bones can be used as an adsorbent to support sustainable development goals (SDGs).

Keywords: Adsorption, calcium carbonate, chicken bone wastes, adsorption isotherm, particles.

1. Introduction

In recent years, the release of toxic compounds, such as dyes by the textile industry into the aquatic environment has caused environmental pollution, and the issue of environmental pollution has become very interesting [1, 2]. This dye is included in one of the main classes as a pollutant because of its toxic, mutagenic, carcinogenic, and non-biodegradable properties [3]. Therefore, an effort is needed to remove the dye in the water. This strategy of removing dyes in water is a practice to reuse water thus it has an impact on reducing costs associated with handling pollution. In addition, this strategy also contributes to environmental protection and public health [4] and is used to support sustainable development goals (SDGs) [5].

Several techniques for treating dye waste in aquatic environments have been tried, for example, conventional techniques and advanced oxidation techniques [6, 7]. However, conventional dye removal techniques are ineffective because dye molecules in industrial water are predominantly neutral or negatively charged [8]. The advanced oxidation process is also regarded as ineffective for dye removal in an aqueous solution because the majority of dyes are photo-stable/biodegradable [6]. Therefore, the adsorption technique is a technique that has proven promising for the treatment of dye effluents. Adsorption is the process by which pollution loads are transferred and/or accumulated from the water phase to the adsorbent phase. This adsorption technique was adopted in this study because of its advantages of being effective, non-selective, and low-cost [9].

Hamzezadeh et al. [6] have reported the ability of Salvia seed-based adsorbents to remove dyes. The results showed that Salvia seeds were suitable for processing aqueous solutions containing dyes, especially for removing cationic blue dye 41 from aqueous solutions. Thus, Salvia seeds can be considered as good absorbent, technically, economically, and environmentally friendly. Polymer-based adsorbent materials such as magnetized chitosan-coated with Fe_2O_3 nanoparticles (C-Fe_2O_3) also have the potential to remove acid blue dye 113. Based on these studies, this polymer-based adsorbent (C-Fe_2O_3) is more effective in treating aqueous solutions containing acid blue dye 113 than other adsorbents [10]. Carbon-based green adsorbents are used to remove dyes from industrial wastes such as malachite green which shows that activated carbon has a significant ability to adsorb dyes due to its high porosity character [11]. Many previous studies also reported the utilization of agricultural waste-based adsorbents as summarized in Table 1 [12-19].

The objective of this research is to assess the isotherm adsorption of calcium carbonate microparticles from chicken bone waste. In contrast to previous studies that only focus on the synthesis and characterization of calcium carbonate, the novelty of this study is the analysis of the adsorption isotherm of calcium carbonate particles from chicken bone waste. Waste is the main focus as a source of calcium carbonate because it has a high amount of calcium carbonate component. In addition, according to the Ministry of Agriculture of the Republic of Indonesia's Directorate General of Animal Husbandry and Animal Health, national production estimates for broiler chicken (broiler) in Indonesia from 2013 to 2017 were 1498.87; 1544.38; 1628.31; 1905.50; and 1848.06 tons, respectively. Increased production of broiler chicken meat appears to be a result of Indonesian people's increasing consumption, increasing the amount of chicken bone waste that is difficult to recycle [20]. Therefore, the development of sustainable raw materials for adsorbent production contributes to a solution to overcome environmental and

economic problems caused by chicken bone waste to support sustainable development goals (SDGs).

Table 1. Previous studies about the use of agricultural waste as an adsorbent for dye degradation treatment.

Sources of adsorbent material	Results	Ref.
Carbon from Pumpkin	According to the findings, the adsorption of pumpkin carbon microparticles on the surface appeared as a monolayer with physical processes.	[12]
Carbon-based Banana Stem Waste	The adsorption process is included in the monolayer with the type of physical adsorption interaction.	[13]
Carbon from Rice Straw	This study demonstrates that using rice straws to make porous carbon particles is effective and that the change in porosity has a direct impact on the product's ability to adsorb molecules.	[14]
Silica from Rice Husk	Silica particles derived from rice husk were found to be effective at adsorbing curcumin molecules. The Freundlich isotherm model is an appropriate adsorption model for this study.	[15]
Carbon from Pineapple Peel Waste	The adsorption profile with carbon particles from pineapple peel waste as an adsorbent follows the Freundlich model that follows multilayer adsorption on heterogeneous surfaces and interactions between adsorbate molecules	[16]
Carbon from Soursop Peel	The size of the particles influences the prediction of the adsorption process. Adsorption of soursop peel waste material occurs on a multilayer surface, with physical adsorption as the adsorbent-adsorbate interaction.	[17]
Carbon from Red Dragon Fruit Peel	The Dubinin-Radushkevich isotherm model is the most appropriate adsorption isotherm model for Red Dragon Fruit Peel Waste as an adsorbent.	[18]
Calcium Carbonate from Barred Fish Bone	The Dubinin-Radushkevich isotherm model is the most appropriate adsorption isotherm model. The findings show that multilayer adsorption occurs at all micrometer sizes and that it involves physical interactions between the adsorbate and the adsorbent surface.	[19]

2. Adsorption isotherm Models

To evaluate the phenomenon during the adsorption process, there are 10 adsorption isotherm models used, including Langmuir, Freundlich, Temkin, Dubinin-Radushkevich, Fowler-Guggenheim, Hill-Deboer, Jovanovic, Harkin-Jura, Flory-Huggins, and Halsey. A possible phenomenon of standard adsorption processes is when adsorption occurs in a monolayer, multilayer, or cooperative manner. Figure 1 shows an illustration of the phenomenon of the monolayer, multilayer, and cooperative adsorption processes. A detailed explanation of the adsorption isotherm model is presented in Fig. 1 [20].

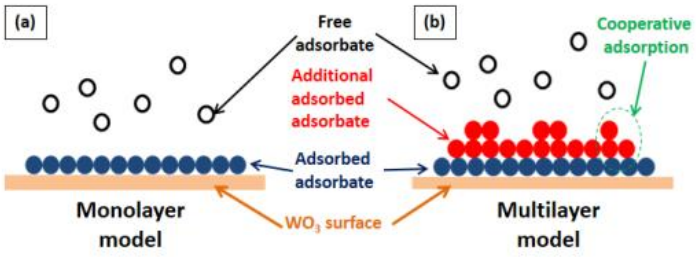

Fig. 1. Illustration of the monolayer, multilayer, and cooperative adsorption process (adapted from reference [21]).

2.1. Langmuir

The Langmuir isotherm is predicated on the adsorption process that takes place on a homogeneous surface that forms a monolayer. Monolayer assumes that the molecules absorbed during the adsorption process do not interact with each other so that they have the same surface energy because no adsorbate transmigrates. This adsorbent's surface monolayer formation prevents further adsorption processes. The Langmuir isotherm equation can be predicted by Eqs. (1) and (2).

$$\frac{1}{Q_e} = \frac{1}{Q_{max} K_L} \frac{1}{C_e} + \frac{1}{Q_{max}} \quad (1)$$

$$R_L = \frac{1}{1+K_L C_e} \quad (2)$$

where K_L is the Langmuir constant, Q_{max} is the adsorption capacity of the monolayer (mg/g), and R_L is the separation factor. Table 2 shows the meaning of the R_L parameter.

Table 2. The meaning of the R_L parameter.

Condition	Explanation
$R_L > 1$	Adsorption is unfavorable because desorption occurs
$R_L = 1$	Adsorption process that is linear and does not depend on the concentration
$R_L = 0$	Irreversible adsorption process because the adsorbate cannot diffuse (usually occurs in chemisorption)

2.2. Freundlich

Freundlich isotherm is based on the adsorption process that occurs on heterogeneous surfaces that form multilayers. Multilayer adsorption allows interactions between adsorbed molecules. Thus, this model implies that the energy is not the same at each surface site. Freundlich's isotherm model can be expressed by Eq. (3).

$$\log Q_e = log k_f + \frac{1}{n} \log C_e \quad (3)$$

where k_f is the Freundlich constant that estimates the adsorption capacity, C_e is the adsorbate concentration at equilibrium (mg/L), n is the degree of nonlinearity, and $1/n$ assumes the adsorption strength. n and $1/n$ parameters have the meaning as shown in Table 3.

Table 3. The meaning of the *n* and 1/*n* parameters.

Condition	Explanation
$n < 1$	Characteristic of the adsorption process with the chemisorption process
$n = 1$	A linear adsorption process with a concentration-independent partition between two phases
$n > 1$	Characteristic of the adsorption process with the physisorption process
$1/n < 1$	Characteristic of the normal process of adsorption
$1/n > 1$	Characteristic of the cooperative process of adsorption
$1 < 1/n < 0$	Characteristic of a favorable process adsorption because there is no desorption process
$0 < 1/n < 1$	Adsorption on heterogeneous surfaces (a 1/*n* value close to 0 indicates that the adsorbent surface is increasingly heterogeneous).

2.3. Temkin

Temkin's isotherm describes the indirect adsorbate interaction when using very low adsorbate concentrations. The heat of adsorption of all molecules in the multilayer is determined by Eq. (4).

$$q_e = B_T ln A_T + B_T ln C_e \quad (4)$$

where A_T and β_T are the equilibrium constants. β_T is explained in Table 4.

Table 4. The meaning of the β_T parameter

Condition	Explanation
$\beta_T < 8$ kJ/mol	Physical adsorption characteristics
$\beta_T > 8$ kJ/mol	Chemical adsorption characteristics

2.4. Dubinin-Radushkevich

The Dubinin-Raduskevich isotherm is based on the assumption that adsorption takes place on heterogeneous surfaces. The adsorption equation of the Dubinin-Radushkevich model is shown by Eq. (5).

$$ln q_e = ln q_s - (\beta \varepsilon^2) \quad (5)$$

where q_s is the theoretical saturation capacity (mg/g), β is the Dubinin-Radushkevich isotherm constant which is correlated with the average free adsorption energy per mole of adsorbate, and ε is the Polanyi potential associated with equilibrium conditions. The Polanyi potential and the calculation of the adsorption energy are expressed by Eq. (6).

$$\varepsilon = RT ln\left[1 + \frac{1}{C_e}\right] \quad (6)$$

Adsorption free energy per adsorbate molecule (E) is calculated using Eq. (7) and the meaning is in Table 5.

$$E = \frac{1}{\sqrt{2\beta}} \quad (7)$$

Table 5. The meaning of the *E* parameter.

Condition	Explanation
$E < 8$ kJ/mol	Physical adsorption characteristics
$E > 8$ kJ/mol	Chemical adsorption characteristics

2.5. Fowler-Guggenheim

The Fowler-Guggenheim isotherm explains that the adsorbed molecules have lateral interactions. The Fowler-Guggenheim isotherm equation is expressed by Eq. (8)

$$K_{FG}C_e = \frac{\theta}{1-\theta}\exp\left(\frac{2.\theta.W}{RT}\right) \quad (8)$$

where K_{FG} is the Fowler-Guggenheim equilibrium constant (L/mg), and W is the interaction energy between the adsorbed molecules (kJ/mol) (see Table 6).

Table 6. The meaning of the *W* parameter

Condition	Explanation
$W > 0$ kJ/mol	Exothermic attraction exists between the adsorbed molecules and the process.
$W < 0$ kJ/mol	Endothermic repulsion exists between adsorbed molecules and the process.
$W = 0$ kJ /mol	There is no interaction between the molecules that have been adsorbed.

2.6. Hill-Deboer

The Hill-de Boer isotherm describes mobile adsorption and the presence of lateral interactions between the molecules that have been adsorbed. The equation for the Hill-de Boer isotherm is expressed by Eq. (9).

$$K_1.C_e = \frac{\theta}{1-\theta}\exp\left(\frac{\theta}{1-\theta} - \frac{K_2\theta}{RT}\right) \quad (9)$$

where K_1 is the Hill-de Boer constant (L/mg), and K_2 is the adsorbed molecular interaction constant. Table 7 shows the meaning of the K_2 parameter.

Table 7. The meaning of the K_2 parameter.

Condition	Explanation
$K_2 > 0$ kJ/mol	Exothermic attraction exists between the adsorbed molecules and the process
$K_2 < 0$ kJ/mol	Endothermic repulsion exists between adsorbed molecules and the process.
$K_2 = 0$ kJ/mol	There is no interaction between the molecules that have been adsorbed

2.7. Jovanovic

The Jovanovic isotherm is predicated on the Langmuir model's phenomena but does not allow mechanical contact between adsorbate and absorbent. Equation (10) depicts the linear equation of the Jovanovic isotherm.

$$lnQ_e = lnQ_{max} - K_jC_e \quad (10)$$

where Q_e is the equilibrium amount of adsorbate in the absorbent (mg/g), Q_{max} is the adsorbate's maximum absorption, and K_J is the Jovanovic constant.

2.8. Harkin-Jura

The Harkin-Jura model assesses adsorption on a heterogeneous surface where the adsorption process takes place by forming a multilayer (see Eq. (11)).

$$\frac{1}{q_e^2} = \frac{B_{HJ}}{A_{HJ}} - \left(\frac{1}{A}\right)logC_e \quad (11)$$

where B_{HJ} is adsorbent specific surface area and A_{HJ} is the Harkin-Jura isotherm constant.

2.9. Flory-Huggins

The Flory-Huggins isotherm considers the adsorbate's surface coverage on the adsorbent and assumes that the adsorption process occurs spontaneously. Equation 12 represents the Flory-Huggins isotherm.

$$log\frac{\theta}{C_e} = logK_{FH} + n\log(1-\theta) \quad (12)$$

where $\theta = (1-\frac{C_e}{C_o})$ which indicates the degree of surface coverage, K_{FH} is the Flory-Huggins isotherm constant, and n_{FH} is the amount of adsorbate occupying the adsorption site. To calculate the Gibbs free energy (ΔG°) of adsorption that occurs spontaneously, the value of ΔG° can be calculated from the equilibrium constant (K_{FH}) which is shown by Eq. (13).

$$\Delta G° = -RTlnK_{FH} \quad (13)$$

The negative value of ΔG° indicates that the adsorption process is spontaneous and depends on temperature.

2.10. Halsey

The Halsey isotherm evaluates adsorption with multilayer characteristics. The equation of the Halsey isotherm is shown by Eq. (14).

$$Q_e = \frac{1}{n_H} lnK_H - \left(\frac{1}{n_H}\right) lnC_e \quad (14)$$

where K_H and n are Halsey's isotherm constants.

The curves of the data fitting result and the calculation of each adsorption isotherm parameter are presented in detail in Table 8.

Furthermore, Eq. (15) is used to calculate the amount adsorbed by the unit mass of the adsorbent at equilibrium (Q_e).

$$Q_e = \frac{C_o - C_e}{m} \times V \quad (15)$$

where C_o is the initial concentration (mg/L), C_e is the equilibrium concentration (mg/L), m is the mass of the adsorbent (g), and V is the volume of the adsorbate solution (L).

3. Method

3.1. Materials

The materials used in this study were chicken bone waste (purchased at the local market in Bandung, Indonesia), pure water, and curcumin (which was obtained by extracting turmeric from a local market in Bandung, Indonesia).

3.2. Preparation of calcium carbonate particles from chicken bone

Samples of chicken bones (about 1000 g) were separated from the meat, washed, and carbonized using an oven at 230°C for 10 hours. After the chicken bone sample was carbonized, to obtain a homogeneous particle size, the chicken bone sample was ground using saw-milling for 2 minutes. Then, the particles were filtered using a sieve test with sieve-mesh hole sizes of 500, 250, 100, 74, and 60 μm.

Table 8. Adsorption isotherm's fitting data, calculation, and parameters.

Isotherm Model	Linear Equation	Plotting		Parameters
		x-Axis	y-Axis	
Langmuir	$\frac{1}{Qe} = \frac{1}{QmaxK_L}\frac{1}{Ce} + \frac{1}{Qmax}$	$^1/_{C_e}$	$^1/_{Q_e}$	• $\frac{1}{Q_{max}} = intercept$ • $K_L = \frac{1}{Q_{max} \times slope}$
Freundlich	$\ln Q_e = \ln k_f + \frac{1}{n}\ln C_e$	lnC_e	lnQ_e	• $lnK_F = intercept$ • $\frac{1}{n} = slope$
Temkin	$q_e = B_T \ln A_T + B_T \ln Ce$	lnC_e	Q_e	• $B = slope$ • $B_T lnA_T = intercept$ • $B_T = \frac{RT}{B}$
Dubinin-Radushkevich	$\ln q_e = \ln q_s - (\beta\varepsilon^2)$	ε^2	lnQ_e	• $\beta = K_{DR} = slope$ • $E = \frac{1}{\sqrt{2 \times K_{DR}}}$
Flory Huggins	$log\frac{\theta}{C_e} = logK_{FH} + n\log(1-\theta)$	$\log\left(\frac{\theta}{C_0}\right)$	$log(1-\theta)$	• $n_{FH} = slope$ • $k_{FH} = intercept$ • $\Delta G^o = RT\ln(k_{FH})$ $\theta = 1 - (\frac{C_e}{C_0})$
Fowler-Guggenheim	$ln\left(\frac{C_e(1-\theta)}{\theta}\right) - \frac{\theta}{1-\theta} = -lnK_{FG} + \frac{2W\theta}{RT}$	θ	$ln\left[\frac{C_e(1-\theta)}{\theta}\right]$	• $W = slope$ • $-lnK_{FG} = intercept$ • $\alpha\ (slope) = \frac{2W\theta}{RT}$ $\theta = 1 - (\frac{C_e}{C_0})$
Hill-Deboer	$ln\left[\frac{C_e(1-\theta)}{\theta}\right] - \frac{\theta}{1-\theta} = -lnK_1 - \frac{K_2\theta}{RT}$	θ	$ln\left[\frac{C_e(1-\theta)}{\theta}\right] - \frac{\theta}{1-\theta}$	• $-lnk_1 = intercept$ • $\alpha\ (slope) = \frac{k_2\theta}{RT}$ • $\theta = 1 - (\frac{C_e}{C_0})$
Jovanovic	$lnq_e = lnq_{max} - K_J C_e$	C_e	lnQ_e	• $K_J = slope$ • $lnq_{max} = intercept$
Harkin-Jura	$\frac{1}{q_e^2} = \frac{B}{A} - \left(\frac{1}{A}\right) logC_e$	$logC_e$	$\frac{1}{q_e^2}$	• $A_H = \frac{1}{Slope}$ • $\frac{B_H}{A_H} = intercept$
Halsey	$lnQ_e = \frac{1}{n_H} lnK_H - \frac{1}{n} lnC_e$	lnC_e	lnQ_e	• $\frac{1}{n} = slope$ • $\frac{1}{n} lnK_H = intercept$

3.3. Physical characterization of calcium carbonate particles

The particle size and morphology of the raw material were investigated using a digital microscope (calcium carbonate from chicken bone waste). To analyze elemental structure products, Fourier transform infrared (FTIR) was used for chemical characterization (FTIR-6600, Jasco Corp.; Japan).

3.4. Batch adsorption experiments

In a beaker glass, 0.05 g of calcium carbonate particles (as adsorbent) were added to 140 mL of curcumin solution with specific concentrations of 100, 80, 60, 40, and 20 ppm (batch experiment). The adsorption test was performed by stirring the curcumin-carbon solution mixture at 1000 rpm for 120 minutes under constant pH environmental conditions (approximately 7). To test adsorption, an aliquot of the mixed solution was taken and filtered through a 0.22 μm pore size nylon membrane syringe filter. After the adsorption process, the concentration of the solution was determined using Visible Spectroscopy (Model 7205; JENWAY; Cole-Parner; US) at maximum wavelengths ranging from 280 to 500 nm. Adsorption data were plotted and normalized. The adsorption results were plotted and normalized. The maximum absorption peak was calculated using Beer's Law to obtain the concentration of curcumin. The obtained concentration data were plotted and compared to the following adsorption isotherm models: Langmuir, Freundlich, Temkin, Dubinin-Radushkevich, Fowler-Guggenheim, Hill-Deboer, Jovanovic, Harkin-Jura, Flory-Huggins, and Halsey. Detailed information for calculating isotherm is in our previous study [20, 21].

4. Results and Discussion

4.1. Physical characteristics of calcium carbonate particles

Figures 2(a**)** and **(**b) show a digital microscope image respectively and Fig. 2(c) is a Ferret analysis of calcium carbonate particles fabricated from chicken bone waste. Figures 2(a**)** and **(**b) show that the calcium carbonate particles have an inhomogeneous size because they have a particle size range from 270-500 μm. Figure 2(c) shows the particle size distribution results where most of the calcium carbonate particles have sizes in the range of 75-100 μm. For information, the average particle size of calcium carbonate is 176 μm.

4.2. Isotherm model-based adsorption characteristics of calcium carbonate particles

The results of fitting the adsorption process with ten adsorption isotherm models are shown in Figs. 3(a)-(j). Based on the data fitting results, three models are suitable to illustrate the adsorption process in this study, respectively, namely Jovanovic, Hill-Deboer, and Fowler-Guggenheim. The suitability of this adsorption model is based on the value of the correlation coefficient (R^2 = 0.95). Table 9 presents detailed data about the correlation coefficient and adsorption parameters. A detailed explanation for each model is discussed as follows.

Figure 3(a) analyses the Langmuir isotherm model which is analyzed based on Eqs. (1) and (2). The adsorption data on the Langmuir isotherm model shows R^2 = 0.732 and the maximum adsorption capacity parameter (Q_{max}) of 4.582 mg/g (see

Table 9). The R_L parameter on the Langmuir isotherm (see Table 1) has a value between 0 and 1, indicating that the adsorption process is profitable [20].

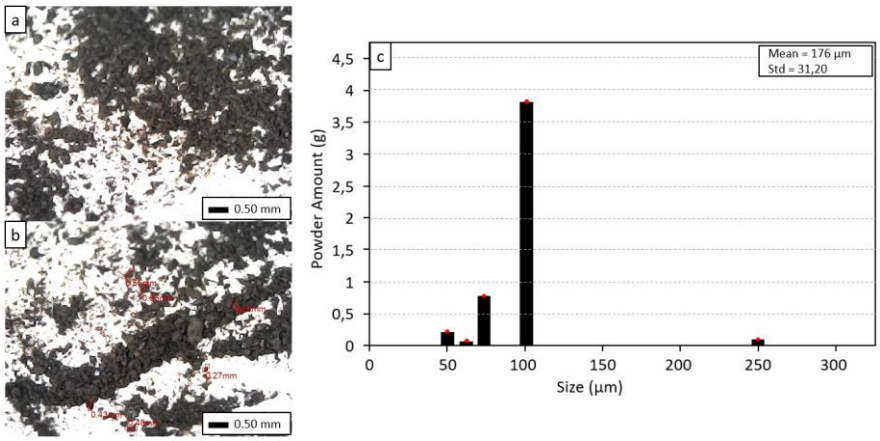

Fig. 2. The digital microscope of calcium carbonate (a)-(b) and Ferret analysis of particle size (c).

Figure 3(b) shows the results of fitting the adsorption data based on Eq. (3). The Freundlich model shows the value of R^2 of 0.8904. The parameter values of n and $1/n$ on the Freundlich isotherm are 1.514 and 0.6601, respectively (see Table 9). Parameter values $n > 1$ and $1/n < 1$ inform that the adsorption process occurs normally, the characteristics of the adsorption process are physical and occur on heterogeneous adsorbent surfaces [20].

Figure 3(c) is studied by plotting the data in Eq. (4). The Temkin model assumes that all molecules on the adsorbent surface have a linearly decreasing heat of adsorption due to uniform energy distribution. The Temkin isotherm model has a value of $R^2 = 0.941$ and a parameter value of T < 8 kJ/mol (see Table 9). Based on the T parameter, the adsorption takes place physically (physisorption) [20].

Figure 3(d) shows the plotting results based on the linear equation (Eq. (5)) of Dubinin-Raduskevich. The Dubinin-Radushkevich isotherm has a value of R^2 = 0.92 and the value of the E parameter is 0.225 (see Table 9). E value < 8 kJ/mol which indicates that the adsorption process is going physically (physisorption) [20].

Figure 3(e) shows the results of plotting analysis based on the Fowler Guggenheim isotherm using Eq. (8). The R^2 value of this equation is 0.9585 and the value of the W parameter is -904,854 kJ/mol (see Table 9). Based on the results of the analysis, the value of $W < 0$ indicates that there is a repulsion between the adsorbed molecules and the process is exothermic [20].

Figure 3(f) is the resulting curve for protecting data on the Hill-Deboer isotherm (Eq. (9)). The Hill-Deboer isotherm has a value of R^2 of 0.9585 with a K_2 parameter value of -1397.129 (see Table 9). Based on the parameter value of K_2 ($K_2 < 0$ kJ/mol), the adsorption process occurs through interactions between molecules that repel each other, and the process is endothermic [20].

Figure 3(g) is the result of plotting data based on the Jovanovic isotherm model using Eq. (10). The values for R^2, A_{HJ}, and B_{HJ} are 0.7066, 18.622, and 1.158

respectively (see Table 9). Based on the results of Jovanovic isotherm plotting, the adsorbent capacity (Q_{max}) is 2.773 (see Table 9). The less Q_{max} value indicates that the adsorbent has a weak adsorption capacity [20].

Figure 3(h) is the Harkin-Jura adsorption model that plots the curve based on Eq. (11). The results of the curve analysis of the Harkin-Jura isotherm show that R^2 is 0.7606 (see Table 9). The Harkin-Jura isotherm parameters identified were A_{HJ} and B_{HJ} parameters. The parameter values for A_{HJ} and B_{HJ} are 18.622 and 1.58, respectively (see Table 9) [20].

The plotting analysis based on Flory-Huggins is shown in Fig. 3(i) (see Eq. (11)). The correlation coefficient (R^2) value of this model is 0.9235 (see Table 9). The presence of interactions between free molecules and adsorbed molecules on the adsorbent's surface was investigated using the n_{FH} parameter value. Because the free molecule attaches to and interacts with the adsorbed molecule, the interaction occurs. This model also informs the Gibbs free energy value. A negative Gibbs free energy parameter indicates that the adsorption process is spontaneous [20].

Figure 3(j) is the result of plotting the data against the Halsey isotherm using Eq. (14). The Halsey isotherm shows the value of R^2 = 0.8904 with the Halsey isotherm constants for K_H and n being 86.981 and 0.6601, respectively (see Table 9) [20].

According to the preceding explanation, an adsorption isotherm is used to find an adsorption model that accurately describes the adsorption. The adsorption isotherm model's suitability was evaluated using the value of the correlation coefficient (R^2). The adsorption isotherm model is more suitable if the R^2 value is close to 1. The order of the adsorption isotherm model suitable for the removal of curcumin dye with calcium carbonate adsorbent is as follows: Jovanovic (R^2 = 0.987) > Hill-Deboer (R^2 = 0.9585) > Fowler-Guggenheim (R^2 = 0.9513) > Temkin (R^2 = 0.941) > Flory-Huggins (R^2 = 0.9235) > Dubinin-Radushkevich (R^2 = 0.92) > Halsey (R^2 = 0.8904) > Freundlich (R^2 = 0.8904) > Harkin-Jura (R^2 = 0.7606) > Langmuir (R^2 = 0.7324). The adsorption results revealed that three adsorption isotherms were unsuitable for describing the adsorption process because the R^2 value is less than 0.9.

The adsorption process followed monolayer adsorption because it had the best match with the Jovanovic isotherm, according to the results of the adsorption process analysis on the most suitable adsorption isotherm model. However, after being confirmed by all other isotherm models with high correlation coefficient values (R^2 > 0.90) including Hill-Deboer, Fowler-Guggenheim, Temkin, Flory-Huggins, and Dubinin-Radushvich, the adsorption process follows multilayer adsorption where the adsorption process occurs on the heterogeneous adsorbent surface (confirmed by the Temkin isotherm) and containing micro-pores (confirmed by the Dubinin-Radushkevich model isotherm).

Although there is a multilayer adsorption formation, the chemical interaction between the adsorbate-adsorbate is weak thus the interaction is physisorption. This physisorption interaction process was confirmed by the isotherm model of Freundlich, Temkin, and Dubinin-Radushkevich. Adsorption by physisorption interactions differs from sublimation in that the adsorbate molecules are attracted to the adsorbent sites by Van der Waals forces, generating slightly more heat than sublimation. Because the adsorption heat is low, less energy was required for desorption [22, 23].

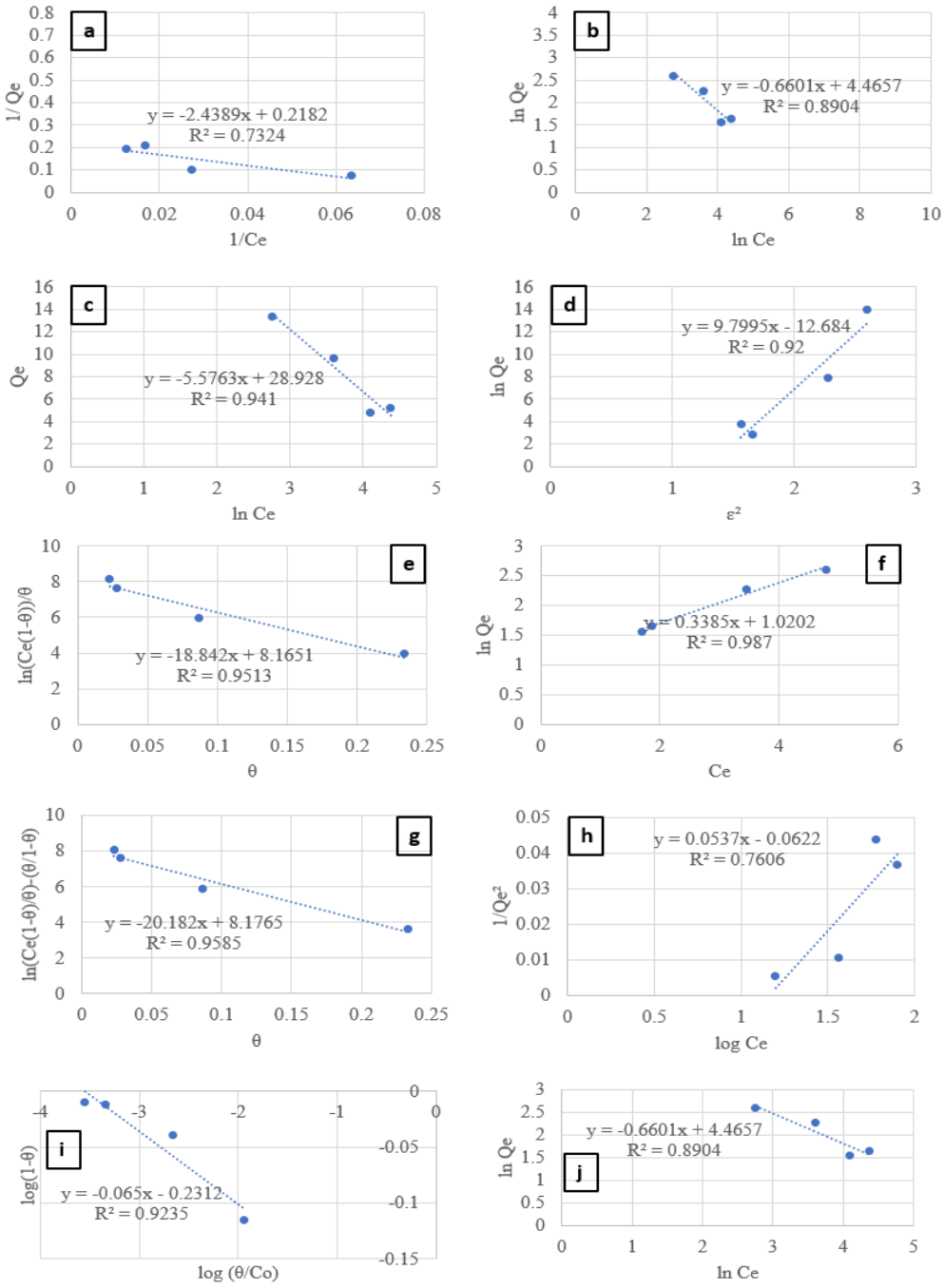

Fig. 3. Data fitting with isotherm models Langmuir (a), Freundlich (b), Temkin (c), Dubinin-Radushkevich (d), Fowler-Guggenheim (e), Hill-Deboer (f), Jovanovic (g), Harkin -Jura (h), Flory-Huggins (i), and Halsey (j).

Table 9. Detailed data of adsorption isotherm parameters.

Model	Parameters	Value	Notes
Langmuir	R^2	0.7324	No monolayer existence on the surface of the adsorbent ($R^2 < 0.90$)
	Q_{max} (mg/g)	4.582	Maximum capacity adsorption
	K_L (L/mg)	0.089	The small value Langmuir constant indicates adsorbate and adsorbent have a weak interaction
	R_L	0.918	Favorable adsorption ($0 < R_L < 1$)
Freundlich	R^2	0.8904	Monolayer existence on the surface of the adsorbent ($R^2 < 0.90$)
	n	1.514	Physisorption ($n > 1$)
	$1/n$	0.6601	Favorable and normal adsorption in heterogeneous surface ($0 < 1/n < 1$)
	K_f (mg/g)	1.935	Adsorbent adsorption capacity
Temkin	R^2	0.941	Uniform distribution adsorbate in the adsorbent surface ($R^2 > 0.90$)
	A_T (L/g)	0.071	Temkin equilibrium binding constant
	β_T (J/mol)	407.03	Physisorption ($\beta_T < 8$ kJ/mol)
Dubinin-Radushkevich	R^2	0.92	The adsorbent surface contains micropores ($R^2 > 0.90$)
	β (mol^2/kJ^2)	9.7995	Dubinin-Radushkevich isotherm constant
	E (kJ/mol)	0.225	Physisorption ($E < 8$ kJ/mol)
Fowler-Guggenheim	R^2	0.9513	No monolayer existence on the surface of the adsorbent ($R^2 > 0.90$)
	W (kJ/mol)	-904.854	$W < 0$ kJ/mol, repulsive interaction between adsorbed molecules
	K_{FG} (L/mg)	284×10^{-4}	Fowler-Guggenheim isotherm constant
Hill-Deboer	R^2	0.9585	No monolayer existence on the surface of the adsorbent ($R^2 > 0.90$)
	K_1 (L/mg)	281×10^{-4}	Hill-Deboer isotherm constant
	K_2 (kJ/mol)	-1397.129	$K_2 < 0$ kJ/mol, Adsorbed molecule repulsive interaction
Jovanovic	R^2	0.987	Monolayer existence on the surface of the adsorbent ($R^2 > 0.90$)
	K_J (L/mg)	0.3385	Jovanovic isotherm constant
	Q_{max} (mg/g)	2.773	Maximum uptake of adsorbate
Harkin-Jura	R^2	0.7606	Multilayer existence on the surface of adsorbent ($R^2 > 0.90$)
	A_{HJ}	18.622	Harkin-Jura isotherm constant
	B_{HJ}	1.158	Related to the surface area of the adsorbent
Flory-Huggins	R^2	0.9235	No monolayer existence on the surface of the adsorbent ($R^2 > 0.90$)
	n_{FH}	0.065	The adsorbate occupies more than one active adsorbent zone ($n_{FH} < 1$)
	K_{FH} (L/mg)	1.702	Flory-Huggins isotherm constant
	$\Delta G°$ (kJ/mol)	-1.207	Spontaneous adsorption ($\Delta G° < 0$)
Halsey	R^2	0.8904	No monolayer existence on the surface of the adsorbent ($R^2 > 0.90$)
	n	1.515	Halsey isotherm constant
	K_H	86.981	Halsey isotherm constant

In addition, overall, the adsorption process was also normal (confirmed by the Freundlich isotherm), spontaneous (confirmed by the Flory-Huggins isotherm), and favorable (confirmed by the Freundlich isotherm). Due to the presence of a multilayer, the adsorbate occupies more than one active adsorbent zone. The adsorption isotherm of curcumin dye by calcium carbonate adsorbent from chicken bone waste is illustrated in Fig. 4.

Based on Fig. 4, all adsorption sites (see section (a) in Fig. 4) are active to absorb free adsorbate molecules (see section (b) in Fig. 4). The porous surface structure of the adsorbent accounts for the presence of multilayer conditions without cooperative interactions (adsorbate-adsorbate molecular interactions) (see section (b) in Fig. 4). The adsorbate molecules interact with one another to form a multilayer (see section (c) in Fig. 4). However, they adhere separately to the adsorbent surface leading to no interaction with each other between the adsorbate molecules (see section (d) in Fig. 4) [22, 23].

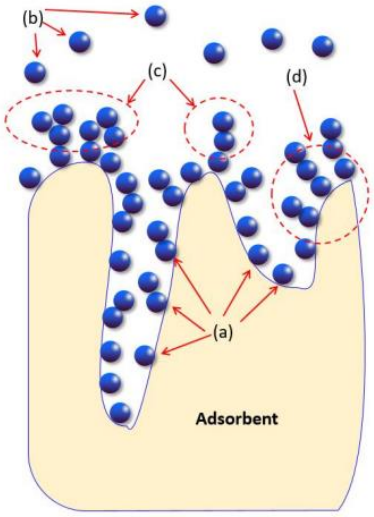

Fig. 4. Adsorption illustration of calcium carbonate in adsorbing adsorbate molecules. The adsorbed molecule on the surface is active; the interaction between adsorbed and free molecules; individually adsorbed molecules in their surface site (separated from each other); and free molecules are represented by (a), (b), (c), and (d), respectively. (Adapted from reference [20]).

5. Conclusion

The adsorption process of the removal of curcumin dye in an aqueous solution with calcium carbonate-based adsorbent from chicken bone waste has been successfully investigated. Sequentially, the adsorption process followed suitability with the Jovanovic isotherm model (R^2 = 0.987) > Hill-Deboer (R^2 = 0.9585) > Fowler-Guggenheim (R^2 = 0.9513) > Temkin (R^2 = 0.941) > Flory-Huggins (R^2 = 0.9235) > Dubinin-Radushkevich (R^2 = 0.92) > Halsey (R^2 = 0.8904) > Freundlich (R^2 = 0.8904) > Harkin-Jura (R^2 = 0.7606) > Langmuir (R^2 = 0.7324). Overall, the adsorption process indicated the formation of multilayers on a uniform (heterogeneous) surface.

Then, the adsorption process occurs normally, spontaneously, and favorably with the interaction between the adsorbate molecules being physical interaction. Adsorption with physisorption interaction has the property of attracting adsorbate molecules to the adsorption site via the Van der Waals force. The additional multilayer without cooperative adsorption confirmed the effect of surface structure (i.e., pores) on adsorption. The findings indicate that an alternative calcium carbonate material derived from chicken bones can be used as an adsorbent to support SDGs.

Acknowledgments

We acknowledged Bangdos Universitas Pendidikan Indonesia.

References

1. Anshar, A.M.; Taba, P.; and Raya, I. (2016). Kinetic and thermodynamics studies the adsorption of phenol on activated carbon from rice husk activated by ZnCl2. *Indonesian Journal of Science and Technology*, 1(1), 47-60.
2. Khelassi-Sefaoui, A.; Khechekhouche, A.; Daouadji, M.Z.D.; and Idrici, H. (2021). Physico-chemical investigation of wastewater from the Sebdou-Tlemcen textile complex North-West Algeria. *Indonesian Journal of Science and Technology*, 6(2), 361-370.
3. Radjenovic, J.; and Sedlak, D.L. (2015). Challenges and opportunities for electrochemical processes as next-generation technologies for the treatment of contaminated water. *Environmental Science and Technology*, 49(19), 11292-11302.
4. Frantz, T.S.; Silveira, N.; Quadro, M.S.; Andreazza, R.; Barcelos, A.A.; Cadaval, T.R.; and Pinto, L.A. (2017). Cu (II) adsorption from copper mine water by chitosan films and the matrix effects. *Environmental Science and Pollution Research*, 24(6), 5908-5917.
5. Maryanti, R.; Rahayu, N.I.; Muktiarni, M.; Al Husaeni, D.F.; Hufad, A.; Sunardi, S.; and Nandiyanto, A.B.D. (2022). Sustainable development goals (SDGs) in science education: Definition, literature review, and bibliometric analysis. *Journal of Engineering Science and Technology*, 17, 161-181.
6. Hamzezadeh, A.; Rashtbari, Y.; Afshin, S.; Morovati, M.; and Vosoughi, M. (2022). Application of low-cost material for adsorption of dye from aqueous solution. *International Journal of Environmental Analytical Chemistry*, 102(1), 254-269.
7. Li, K.; Li, P.; Cai, J.; Xiao, S.; Yang, H.; and Li, A. (2016). Efficient adsorption of both methyl orange and chromium from their aqueous mixtures using a quaternary ammonium salt modified chitosan magnetic composite adsorbent. *Chemosphere*, 154, 310-318.
8. Oladipo, A.A.; and Ifebajo, A.O. (2018). Highly efficient magnetic chicken bone biochar for removal of tetracycline and fluorescent dye from wastewater: two-stage adsorber analysis. *Journal of Environmental Management*, 209, 9-16.
9. Shirmardi, M.; Khodarahmi, F.; Heidari Farsani, M.; Naeimabadi, A.; Vosughi Niri, M.; and Jafari, J. (2012). Application of oxidized multiwall carbon nanotubes as a novel adsorbent for removal of Acid Red 18 dye from

aqueous solution. *Journal of North Khorasan University of Medical Sciences*, 4(3), 335-346.

10. Al-Musawi, T.J.; Mengelizadeh, N.; Al Rawi, O.; and Balarak, D. (2022). Capacity and modeling of acid blue 113 dye adsorption onto chitosan magnetized by Fe_2O_3 nanoparticles. *Journal of Polymers and the Environment*, 30(1), 344-359.
11. El-Bindary, M.A.; El-Desouky, M.G.; and El-Bindary, A.A. (2022). Adsorption of industrial dye from aqueous solutions onto thermally treated green adsorbent: A complete batch system evaluation. *Journal of Molecular Liquids*, 346, 117082.
12. Nandiyanto, A.B.D.; Hofifah, S.N.; Inayah, H.T.; Putri, S.R.; Apriliani, S.S.; Anggraeni, S.; and Rahmat, A. (2021). Adsorption isotherm of carbon microparticles prepared from pumpkin (Cucurbita maxima) seeds for dye removal. *Iraqi Journal of Science*, 62(5), 1404-1414.
13. Nandiyanto, A.B.D.; Azizah, N.N.; and Rahmadianti, S. (2021). Isotherm study of banana stem waste adsorbents to reduce the concentration of textile dying waste. *Journal of Engineering Research*, 9(ASSEEE Special Issue), 1-15.
14. Nandiyanto, A.B.D.; Putra, Z.A.; Andika, R.; Bilad, M.R.; Kurniawan, T.; Zulhijah, R.; and Hamidah, I. (2017). Porous activated carbon particles from rice straw waste and their adsorption properties. *Journal of Engineering Science and Technology* (*JESTEC*), 12(8), 1-11.
15. Ragadhita, R.; Nandiyanto, A.B.D.; Nugraha, W.C.; and Mudzakir, A. (2019). Adsorption isotherm of mesopore-free submicron silica particles from rice husk. *Journal of Engineering Science and Technology* (*JESTEC*), 14(4), 2052-2062.
16. Nandiyanto, A.B.D.; Girsang, G.C.S.; Maryanti, R.; Ragadhita, R.; Anggraeni, S.; Fauzi, F.M.; Sakinah, P.; Astuti, A.P.; Usdiyana, D.; Fiandi, M.; Dewi, M.W.; and Al-Obaidi, A.S.M. (2020). Isotherm adsorption characteristics of carbon microparticles prepared from pineapple peel waste. *Communications in Science and Technology*, 5(1), 31-39.
17. Nandiyanto, A.B.D.; Arinalhaq, Z.F.; Rahmadianti, S.; Dewi, M.W.; Rizky, Y.P.C.; Maulidina, A.; Anggraeni, S.; Bilad, M.R.; and Yunas, J. (2020). Curcumin adsorption on carbon microparticles: synthesis from soursop (AnnonaMuricata L.) peel waste, adsorption isotherms and thermodynamic and adsorption mechanism. *International Journal of Nanoelectronics and Materials* (*IJNeaM*), 13, 173-192.
18. Nandiyanto, A.B.D.; Maryanti, R.; Fiandini, M.; Ragadhita, R.; Usdiyana, D.; Anggraeni, S.; Arwa, W.R.; and Al-Obaidi, A.S.M. (2020). Synthesis of carbon microparticles from red dragon fruit (Hylocereus undatus) peel waste and their adsorption isotherm characteristics. *Molekul*, 15(3), 199-209.
19. Nandiyanto, A.B.D.; Erlangga, T.M.S.; Mufidah, G.; Anggraeni, S.; Bilad, R.; and Yunas, J. (2020d). Adsorption isotherm characteristics of calcium carbonate microparticles obtained from barred fish (Scomberomorus spp.) bone using two-parameter multilayer adsorption models. *International Journal of Nanoelectronics and Materials* (*IJNeaM*), 13, 45-57.

20. Ragadhita, R.; and Nandiyanto, A.B.D. (2021). How to calculate adsorption isotherms of particles using two-parameter monolayer adsorption models and equations. *Indonesian Journal of Science and Technology*, 6(1), 205-234.
21. Nandiyanto, A.B.D.; Ragadhita, R.; and Yunas, J. (2020). Adsorption Isotherm of densed monoclinic tungsten trioxide nanoparticles. *Sains Malaysiana*, 49(12), 2881-2890.
22. Berger, A.H.; and Bhown, A.S. (2011). Comparing physisorption and chemisorption solid sorbents for use separating CO_2 from flue gas using temperature swing adsorption. *Energy Procedia*, 4, 562-567.
23. Nandiyanto, A.B.D. (2020). Isotherm adsorption of carbon microparticles prepared from pumpkin (Cucurbita maxima) seeds using two-parameter monolayer adsorption models and equations. *Moroccan Journal of Chemistry*, 8(3), 8-3.